Enhanced boron rejection of a thin-film composite membrane by embedding additives including hydroxyl groups

Hee Ro Chae[a], Deok-Ro Lee[a], In-Chul Kim[a,*], Young-Nam Kwon[b,*]

[a]*Center for Membrane, Advanced Green Chemical Materials Division, Korea Research Institute of Chemical Technology, Daejeon 34114, Republic of Korea, Tel. +82-42-860-7638; email: ickim@krict.re.kr (I.-C. Kim), Tel. +82 42-610-8592; email: chr0619@krict.re.kr (H.R. Chae), Tel. +82 42-860-7040; email: shine9100@naver.com (D.-R. Lee)*
[b]*School of Urban and Environmental Engineering, Ulsan National Institute of Science and Technology (UNIST), Ulsan 44919, Republic of Korea, Tel. +82-52-217-2810; email: kwonyn@unist.ac.kr (Y.-N. Kwon)*

ABSTRACT

Herein, (±)-3-amino-1,2-propandiol (APD) and N-methyl-D-glucamine (NMDG), which have hydroxyl groups, were respectively embedded in thin-film composite (TFC) membranes to enhance boron rejection. The membranes prepared with embedding materials (APD or NMDG) that are involved in interfacial polymerization showed an increased degree of crosslinking, which was confirmed by X-ray photoelectron spectrometry, causing a decrease of surface roughness and water flux. However, the APD and NMDG bound to the inside of the active layer enhanced boron rejection of the TFC membrane to 85.5% and 87.7%, respectively, at pH 8 due to tightening of membrane pores by the enhanced degree of crosslinking and complex formation of the additives with boric acid.

Keywords: Boron rejection; Reverse osmosis; Thin-film composite membrane

1. Introduction

There is a growing demand for cost and energy efficient membrane technology in water treatment processes. In particular, reverse osmosis (RO) membranes are widely used in the field of seawater desalination [1,2]. The economic advantage of water treatment processes using the membrane originate from the development of highly permselective thin-film composite (TFC) membranes and the development of energy recovery devices, and thus most RO processes adopt a TFC membrane [3,4]. Although researches on seawater desalination membranes have been ongoing for more than 50 years, most of studies have focused on improving salt rejection and developing high permeable membranes. There are areas that still require research [5,6], including in particular the development of membrane technology to satisfy the water quality standards of boron in the field of seawater desalination [7,8].

A small amount of boron is essential for human health, whereas boron is dangerous when taken in excess [9]. The World Health Organization (WHO) established a drinking-water guideline of 0.3 mg/L for boron in 1993. However, it was difficult to satisfy the standard in areas with high boron levels, and therefore the standard was raised to 0.5 mg/L [8]. Since WHO standards are based solely on human health, the standard was adjusted again in 2009 to 2.4 mg/L. When the boron intakes of other animals and plants are taken into account, the limits for boron level vary from 0.5 to 5.0 mg/L [10].

Boron exists in the form of boric acid or borate in the aqueous system. The typical pK_a value of boron is 9.2 at normal conditions (20°C, atmospheric pressure). When pH is

* Corresponding authors.

below or above the pK_a value, boron exists as boric acid or borate, respectively. At the pH of seawater (pH of 8.0–8.3) [11], about 88.8%–94.1% of boron is in the form of neutral boric acid, which is not significantly hydrated by water and thus has small size [12]. The neutral compounds are generally difficult to remove compared to ionic compounds. One approach to improve boron rejection in seawater desalination is to raise the pH of the feed solution above pK_a [9,10]. When the pH value is above 10.2, most of the boron (~90%) becomes borate with a negative charge, and thus boron rejection can be significantly enhanced due to the relatively large hydration radius of borate and electrostatic repulsion between negatively charged borate and the membrane surface. Given the treatment capacity of the seawater desalination process, where a large amount of seawater must be handled, adjusting the pH of seawater to control the boron rejection is not economically feasible. In recent studies, TFC membranes have been developed for increasing boron rejection. Hu et. al. [13] reacted with trimesoyl chloride (TMC) and a sulfonated diamine monomer, 4,4'-(1,2-ethanediyldiimino)bis(benzenesulfonic acid), to form an interfacial layer on a poly(ether sulfone) substrate, and prepared a charge-aggregate induced RO membrane having high boron rejection. La et al. [14] prepared bilayer polyamide (PA) to achieve high boron rejection using sequential interfacial polymerization (SIP), which consists of two polymerization steps in series. They reacted a hexafluoroalcohol-containing diamine with the unreacted TMC moiety of the polyamide active surface. Similar to La et al [14] and Vincenzo et. al. [15] slightly improved boron rejection by bounding amino polyols to the active surface of PA using SIP.

In this study, a TFC membrane was fabricated via the embedment of additives having a hydroxyl group inside the PA active layer in order to enhance boron rejection of the membrane. (±)-3-amino-1,2-propandiol (APD) and N-methyl-D-glucamine (NMDG) were chosen (Fig. 1) as embedding additives, and the effects of the embedding material (APD or NMDG) added during the interfacial polymerization on the physico-chemical properties and performance (especially boron rejection) were investigated.

2. Materials and methods

2.1. Materials

APD and NMDG (Sigma-Aldrich, USA) were used as additives. m-phenylene diamine (MPD) (DuPont, USA), (TMC, Sigma-Aldrich, USA), and isoparaffin (ISOL-C, SK
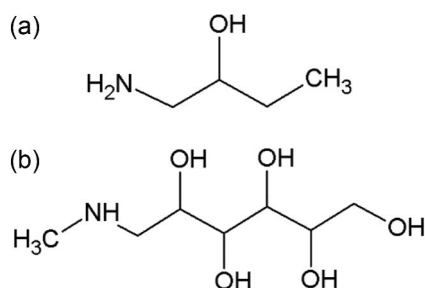
Chemical, Korea) were used to fabricate a PA active layer of a TFC membrane. A PSf ultrafiltration membrane (LG Chem., Korea) was used as the support membrane for interfacial polymerization. Boric acid (Sigma-Aldrich, USA) and sodium chloride (NaCl, Samchun Chemical, Korea) were employed to evaluate the membrane performance. Sodium hydroxide (NaOH, Samchun Chemical, Korea) was applied to adjust the pH of the feed solution.

2.2. Fabrication of control, APD, and NMDG membranes

The TFC membranes were prepared via interfacial polymerization on the PSf support membrane. The PSf support membrane was immersed in a 3.0 wt.% MPD aqueous solution for 2 min. Thereafter, the excess MPD solution remaining on the support membrane was removed using a pressure roller of 5 bar for ~0.5 min and then the support membrane was immersed in a 0.15 wt.% TMC solution (in ISOL-C) for 1 min to form a PA active layer via interfacial polymerization. The prepared TFC membrane was subsequently dried in an oven at 60°C for 10 min and then immersed in deionized water at 40°C for at least 90 min to wash off the unreacted materials. For the preparation of a PA TFC membrane providing enhanced boron rejection, interfacial polymerization proceeded after adding 0.2 wt.% of APD or NMDG to the MPD aqueous solution. The membranes are denoted as APD and NMDG membranes, respectively.

2.3. Characterization of control, APD, and NMDG membranes

The elemental ratio of the PA active layer was evaluated by X-ray photoelectron spectrometry (XPS, Axis nova, Kratos). The surface morphology of the TFC membranes was observed by field-emission scanning electron microscopy (SEM, Carl Zeiss, SigmaHD) and atomic force microscopy (AFM, Nanoscope V, Bruker, Santa Barbara, CA, USA). SEM images were taken after a platinum coating was deposited on the TFC membranes with a sputter coater (Sputter Coater 108, Cressington, UK). The AFM was operated in tapping mode at a 0.8 Hz scanning rate over a scan range of 5.0×5.0 μm^2. The surface hydrophilicity of the TFC membranes was measured by a contact angle analyzer (Phoenix 300, SEO) with a 5.0 µL DI water drop using the sessile drop method. All of the characterizations were conducted after the TFC membranes were dried in air for 24 h.

2.4. Filtration tests of control, APD, and NMDG membranes

The permselectivity of the TFC membranes was evaluated using a cross-flow system at 800 psi for 30 min after 1 h of conditioning. The temperature was maintained at 25°C using a low-temperature bath/circulator (RW-0525G, Lab Companion, Korea). During the last 10 min of each run, the sample was collected. The feed solution is composed as follows: pH of 8, 5 mg/L boron, and 32,000 ppm NaCl. The pH of the feed solution was adjusted by a diluted NaOH solution. The concentration of salt and boron in the feed and permeate was measured by a portable conductivity meter (ORION STAR A222, Thermo Scientific) and an inductively coupled plasma-atomic emission spectrometer (ICP-AES, iCAP 7400 duo, Thermo Scientific, Waltham, MA, USA), respectively.

Fig. 1. Molecular structures of (a) APD and (b) NMDG.

3. Results and discussion

3.1. Characterization of control, APD, and NMDG membranes

The atomic percent of carbon (C), oxygen (O), and nitrogen (N) and atomic percent ratio of N to O of the PA active layer of the TFC membranes was investigated using XPS (Table 1). It is well known that a PA active layer consists of a crosslinked portion ($C_{18}H_{12}N_3O_3$) containing one more amide linkage and a linear portion ($C_{15}H_{10}N_2O_4$) possessing free pendant carboxylic acid groups [16–18]. Theoretically, the PA active layer is entirely crosslinked at a nitrogen/oxygen (N/O) ratio of 1.0, whereas the PA active layer is entirely linear at a N/O ratio of 0.5 [Eq. (2)]. The degree of crosslinking of the PA active layer can be evaluated by the N/O ratio.

$$m + n = 1 \qquad (1)$$

$$\frac{N}{O} = \frac{(3m + 2n)}{(3m + 4n)} \qquad (2)$$

where m and n are the crosslinking and linear portions of PA, respectively, and thus the sum of m and n is 1 (Eq. 1). The degree of crosslinking becomes high when the N/O ratio is increased. The N/O ratios of the control, APD, and NMDG membranes were 0.81, 0.92, and 0.89, respectively (Table 1). Therefore, the sequence of degree of crosslinking was APD > NMDG > control membranes. It appears that the cause of increment of the degree of crosslinking is that additional amine and hydroxyl groups of APD and NMDG can react with TMC during the interfacial polymerization. The reason for the higher degree of crosslinking at APD than at

NMDG might be high mobility [19] and low steric hindrance [20] due to its small size.

The surface roughness of the TFC membrane was reduced by the embedment of NMDG and the roughness was decreased more by the embedment of APD (Table 2). The decrease of the surface roughness was likely due to the increment in the degree of crosslinking of PA [17,21]. The surface roughness of the most crosslinked APD membrane was the lowest among the TFC membranes.

The reduction of the surface roughness was also observed in SEM images (Fig. 2). On the NMDG membrane, the number and the size of ridges were slightly decreased, and thus more dark ground (Fig. 2c) appeared compared to the control membrane (Fig. 2a). On the APD membrane, the number and the size of ridges were substantially reduced, and thus the bright protrusive parts almost disappeared (Fig. 2b) [22].

The effect of additives of APD and NMDG was also investigated using Fourier-transform infrared spectroscopy (FTIR). However, there was no noticeable difference between the FTIR spectra of APD/NMDG and control polyamide membrane (data not shown). This is likely because the –OH/–NH functional groups and aliphatic carbon (Fig. 1) peaks of APD and NMDG are already possessed by the control membrane, and the peaks resulted from the additives appear to be overlapped with the peaks of control membrane

3.2. Membrane performance of the TFC membrane

3.2.1. Water permeance

The water permeance of the APD and NMDG membranes was decreased by 11% and 15%, respectively, compared to that of the control membrane (Table 3). The decreased water permeance of the additive-embedded membranes

Table 1
Atomic percent of elements and N/O ratio of the TFC membranes ($n = 3$)

TFC membrane	C (%)	O (%)	N (%)	N/O ratio
Fully linear	71.4	19.1	9.5	0.50
Fully crosslinked	75.0	12.5	12.5	1.00
Control	77.3	12.4	10.1	0.81
APD	76.2	12.4	11.4	0.92
NMDG	73.8	13.9	12.3	0.89

Table 2
Average roughness (R_a) of the TFC membranes ($n = 3$)

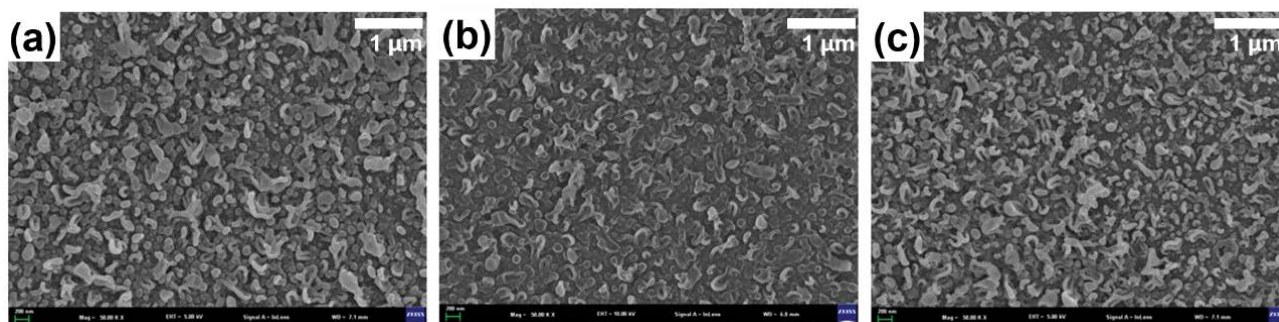| TFC membrane	Average roughness (nm)
Control	63.7 ± 4.2
APD	35.2 ± 1.9
NMDG	47.3 ± 1.4

Fig. 2. Top view SEM images of (a) control, (b) APD, and (c) NMDG membranes at 50,000× magnification.

Table 3
Water permeance and contact angle of the TFC membranes (n = 3)

TFC membrane	Permeance (L m^{-2} h^{-1} bar^{-1})	Contact angle (°)
Control	0.72 ± 0.07	67.7 ± 1.6
APD	0.65 ± 0.03	68.0 ± 3.6
NMDG	0.61 ± 0.03	71.8 ± 1.1

may be caused by the lowered surface roughness [23] and the enhanced degree of crosslinking of PA [24]. The membrane water permeance is generally proportional to the surface roughness and is inversely proportional to degree of crosslinking of PA. Meanwhile, the water permeance of the NMDG membrane was lower than that of the APD membrane, although the degree of reduced roughness and enhanced crosslinking was respectively smaller in the NMDG membrane. This might be due to the hydrophobicity of the NMDG membrane. It is well known that the hydrophobicity of a TFC membrane is inversely proportional to the membrane water permeance [25]. The NMDG membrane was more hydrophobic compared to the control and APD membranes (Table 3).

3.2.2. Salt rejection and boron rejection

The salt rejection of the TFC membranes is shown in Table 4. The salt rejections of the APD and NMDG membranes was respectively slightly higher than that of the control membrane, because the PA active layer of the APD and NMDG membranes was more crosslinked than that of the control membrane. A more crosslinked PA active layer has higher salt rejection [26,27], indicating the APD and NMDG membranes have a smaller pore size than the control membrane.

At the pH of seawater (pH ~ 8), the dominant species of boron is a neutral boric acid. The neutral boric acid is difficult to separate compared to the other species (borate) due to the small hydration size of boric acid and the absence of electrostatic repulsion interaction with the membrane surface. In this study, however, the boron rejection of the APD and NMDG membranes was 85.5% and 87.7%, respectively (Table 4). In comparison with the control membrane, the APD and NMDG membranes exhibited 3.14% and 5.30% higher boron rejection, respectively. The improved boron rejection may be caused by interaction between boric acid and the hydroxyl groups of the additives and also the smaller pore size of the APD and NMDG membranes. Joshi et al. [28] reported that hydroxyl groups (i.e. cis diols) bind with boron species efficiently and selectively to form

Table 4
Salt and boron rejection of the TFC membranes (n = 3)

TFC membrane	Salt rejection (%)	Boron rejection (%)
Control	99.20 ± 0.18	82.35 ± 2.04
APD	99.40 ± 0.10	85.49 ± 0.39
NMDG	99.51 ± 0.08	87.65 ± 1.38

complexes. Kaftan et al. [29] used boron adsorption capability of a polymer containing –OH functional groups for the development of a sorbent for boron from an aqueous solution. The NMDG enhanced boron rejection more than APD because it had more hydroxyl groups than APD at the same weight. Moreover, it is well known that the smaller pore size induces higher boron rejection.

APD and NMDG, which can form a complex with boron, can be bound to the active surface of a PA membrane by post-treatment of an already fabricated PA membrane, but the complex forming sites may be limited in this case. However, participation of the embedding materials (APD and NMDG) in the interfacial polymerization with TMC can expose the embedding materials to the feed solution in the whole body of the active layer. Therefore, the one-step embedding methods proposed in this study could be a better option than surface modification applied as a post treatment. Furthermore, when the embedding method is applied, APD and NMDG can be involved in interfacial polymerization, increasing the degree of crosslinking of the membrane and decreasing the pore size, subsequently improving rejection of boron and ions.

Finally, the water permeance and the boron rejection of the prepared TFC membranes were compared to those of other membranes in previous studies [7,8,30–32] (Fig. 3). The boron rejection of the NMDG membrane was the highest, but its water permeance was quite low in comparison with previous studies because water permeance is inversely proportional to boron rejection [33]. However, the water permeance of the APD and NMDG membranes was relatively good among the membranes having boron rejection of 75% or more. The additives embedding in the polyamide membrane decreased the roughness (Fig. 2.) of membrane surface and increased the degree of crosslinking (Table 1), resulting in the decrease of water permeance as shown in Fig. 3. However, it seems that the reduced crosslinking degree and complex formation of boron with hydroxyl groups in the additives [28, 29] increased the boron rejection.
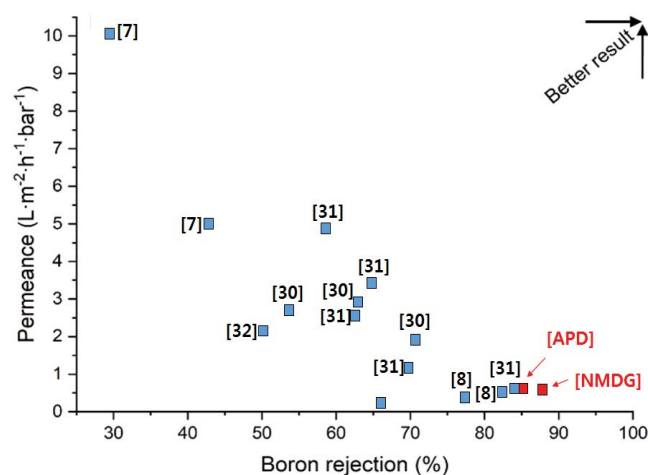

Fig. 3. Water permeance and boron rejection reported in previous studies and those of membranes developed in current study (at pH 8).

H. R. Chae et al. / Desalination and Water Treatment 162 (2019) 112–116

4. Conclusions

In this work, the effect of APD and NMDG, which have hydroxyl functional groups and participate in the interfacial polymerization of the polyamide membrane, on boron rejection was investigated. The addition of APD or NMDG as embedding materials of a TFC PA membrane decreased roughness and water permeability by leading to further crosslinking of polymers on the surface layer of the membrane. The APD and NMDG improved boron rejection up 85.5% and 87.7%, respectively, by the formation of small pore size and complex formation with boron species. Furthermore, the water permeability of embedding membranes was relatively high compared with the membranes providing boron rejection of more than 75%. This experiment shows the usage of additives having hydroxyl functional groups as embedding materials of a TFC membrane can improve the boron rejection.

Acknowledgements

References

[1] I.G. Wenten, Khoiruddin, Reverse osmosis applications: prospect and challenges, Desalination, 391 (2016) 112–125.
[2] L.F. Greenlee, D.F. Lawler, B.D. Freeman, B. Marrot, P. Moulin, Reverse osmosis desalination: water sources, technology, and today's challenges, Water Res., 43 (2009) 2317–2348.
[3] I.C. Escobar, E.M. Hoek, C.J. Gabelich, F.A. DiGiano, Y.A. Le Gouellec, P. Berube, K.J. Howe, J. Allen, K.Z. Atasi, M.M. Benjamin, P.J. Brandhuber, J. Brant, Y.-J. Chang, M. Chapman, A. Childress, W.J. Conlon, T.H. Cooke, I.A. Crossley, G.F. Crozes, P.M. Huck, S.N. Kommineni, J.G. Jacangelo, A.A. Karimi, J.-H. Kim, D.F. Lawler, Q.L. Li, L.C. Schideman, S. Sethi, J.E. Tobiason, T. Tseng, S. Veerapaneni, A.K. Zander, Committee report: recent advances and research needs in membrane fouling, J. Am. Water Works Assn., 97 (2005) 79–89.
[4] M. Said, S. Ebrahim, A. Gad, S. Kandil, Toward energy efficient reverse osmosis polyamide thin-film composite membrane based on diaminotoluene, Desal. Wat. Treat., 71 (2017) 261–270.
[5] W.J. Lau, A.F. Ismail, N. Misdan, M.A. Kassim, A recent progress in thin film composite membrane: a review, Desalination, 287 (2012) 190–199.
[6] P.W. Morgan, Condensation polymers: by interfacial and solution methods, Polym. Rev., 10 (1965) 19–64.
[7] P. Dydo, I. Nemś, M. Turek, Boron removal and its concentration by reverse osmosis in the presence of polyol compounds, Sep. Purif. Technol., 89 (2012) 171–180.
[8] Y. Cengeloglu, G. Arslan, A. Tor, I. Kocak, N. Dursun, Removal of boron from water by using reverse osmosis, Sep. Purif. Technol., 64 (2008) 141–146.
[9] K.L. Tu, L.D. Nghiem, A.R. Chivas, Coupling effects of feed solution pH and ionic strength on the rejection of boron by NF/RO membranes, Chem. Eng. J., 168 (2011) 700–706.
[10] N. Kabay, M. Bryjak, N. Hilal, Boron Separation Processes, Elsevier, Amsterdam, 2015.
[11] G.M. Marion, F.J. Millero, M.F. Camões, P. Spitzer, R. Feistel, C.-T.A. Chen, pH of seawater, Mar. Chem., 126 (2011) 89–96.
[12] N.N. Greenwood, A. Earnshaw, Chemistry of the Elements, 2nd ed., Butterworth-Heinemann, Oxford, 1997.
[13] J. Hu, Y. Pu, M. Ueda, X. Zhang, L. Wang, Charge-aggregate induced (CAI) reverse osmosis membrane for seawater desalination and boron removal, J. Membr. Sci., 520 (2016) 1–7.
[14] Y.-H. La, J. Diep, R. Al-Rasheed, D. Miller, L. Krupp, G.M. Geise, A. Vora, B. Davis, M. Nassar, B.D. Freeman, M. McNeil, G. Dubois, Enhanced desalination performance of polyamide bi-layer membranes prepared by sequential interfacial polymerization, J. Membr. Sci., 437 (2013) 33–39.
[15] M. Di Vincenzo, M. Barboiu, A. Tiraferri, Y.M. Legrand, Polyol-functionalized thin-film composite membranes with improved transport properties and boron removal in reverse osmosis, J. Membr. Sci., 540 (2017) 71–77.
[16] Y.-N. Kwon, C.Y. Tang, J.O. Leckie, Change of chemical composition and hydrogen bonding behavior due to chlorination of crosslinked polyamide membranes, J. Appl. Polym. Sci., 108 (2008) 2061–2066.
[17] C.N. Grover, J.H. Gwynne, N. Pugh, S. Hamaia, R.W. Farndale, S.M. Best, R.E. Cameron, Crosslinking and composition influence the surface properties, mechanical stiffness and cell reactivity of collagen-based films, Acta Biomater., 8 (2012) 3080–3090.
[18] Y.-N. Kwon, R. Joksimovic, I.-C. Kim, J.O. Leckie, Effect of bromide on the chlorination of a polyamide membrane, Desalination, 280 (2011) 80–86.
[19] M. Stanley, An Introduction to Fluid Dynamics: Principles of Analysis and Design, Wiley, Hoboken, New Jersey, 1998.
[20] M.H. Joseph, Organic Chemistry, 2nd ed., Thomson Brooks Cole, Boston, MA, 2005.
[21] G. Mabilleau, I.C. Stancu, T. Honoré, G. Legeay, C. Cincu, M.F. Baslé, D. Chappard, Effects of the length of crosslink chain on poly(2-hydroxyethyl methacrylate) (pHEMA) swelling and biomechanical properties, J. Biomed. Mater. Res. Part A, 77A (2005) 35–42.
[22] R. Shimizu, T.E. Everhart, N.C. MacDonald, C.T. Hovland, Edge effect in high-resolution scanning Auger-electron microscopy, Appl. Phys. Lett., 33 (1978) 549–551.
[23] M. Hirose, H. Ito, Y. Kamiyama, Effect of skin layer surface structures on the flux behaviour of RO membranes, J. Membr. Sci., 121 (1996) 209–215.
[24] B. Bolto, T. Tran, M. Hoang, Z. Xie, Crosslinked poly(vinyl alcohol) membranes, Prog. Polym. Sci., 34 (2009) 969–981.
[25] G.N.B. Baroña, J. Lim, M. Choi, B. Jung, Interfacial polymerization of polyamide-aluminosilicate SWNT nanocomposite membranes for reverse osmosis, Desalination, 325 (2013) 138–147.
[26] L.Y. Hung, C.C. Hu, W.S. Hung, S.J. Lue, Probing free volume property of polyamide thin film composites with different cross-linking densities, MOJ Polym. Sci., 2 (2018) 1–4.
[27] G.-D. Kang, C.-J. Gao, W.-D. Chen, X.-M. Jie, Y.-M. Cao, Q. Yuan, Study on hypochlorite degradation of aromatic polyamide reverse osmosis membrane, J. Membr. Sci., 300 (2007) 165–171.
[28] M.D. Joshi, G. Chalumot, Y.-w. Kim, J.L. Anderson, Synthesis of glucaminium-based ionic liquids and their application in the removal of boron from water, Chem. Commun., 48 (2012) 1410–1412.
[29] O. Kaftan, M. Açıkel, A.E. Eroğlu, T. Shahwan, L. Artok, C.Y. Ni, Synthesis, characterization and application of a novel sorbent, glucamine-modified MCM-41, for the removal/preconcentration of boron from waters, Anal. Chim. Acta, 547 (2005) 31–41.
[30] P. Dydo, M. Turek, J. Ciba, J. Trojanowska, J. Kluczka, Boron removal from landfill leachate by means of nanofiltration and reverse osmosis, Desalination, 185 (2005) 131–137.
[31] H. Koseoglu, B.I. Harman, N.O. Yigit, E. Guler, N. Kabay, M. Kitis, The effects of operating conditions on boron removal from geothermal waters by membrane processes, Desalination, 258 (2010) 72–78.
[32] E. Yavuz, Ö. Arar, M. Yüksel, Ü. Yüksel, N. Kabay, Removal of boron from geothermal water by RO system-II-effect of pH, Desalination, 310 (2013) 135–139.
[33] K.L. Tu, A.R. Chivas, L.D. Nghiem, Effects of chemical preservation on flux and solute rejection by reverse osmosis membranes, J. Membr. Sci., 472 (2014) 202–209.